The European heat wave 2003: Early indicators from multisensoral microwave remote sensing?

Alexander Loew,[1] Thomas Holmes,[2] and Richard de Jeu[2]

Received 3 June 2008; revised 25 September 2008; accepted 21 November 2008; published 4 March 2009.

[1] An extreme heat wave affected large parts of Europe in 2003 with severe socioeconomic impacts. The extreme warm weather conditions lasted over a couple of months with positive temperature anomalies of 5°C for large parts of Europe. Simulations of the event using regional climate models revealed that a pronounced precipitation deficit in the beginning of the year, together with an early onset of the vegetation, resulted in a severe deficit of the soil water content. This amplified the course of the heat wave due to an increasing sensible heat flux from the land surface. The monitoring of temporal and spatial dynamics of soil water content can be accomplished using remote-sensing-based techniques. The present paper addresses the question whether there have been early indicators for the low soil water content using either physically based land surface modeling or remote-sensing-based monitoring techniques. The course of the spring surface soil moisture evolution is investigated using observations from two different microwave remote sensing sensors. An intercomparison of the high-resolution data from the European ENVISAT satellite and coarse resolution data from the AMSR-E mission is made. Remote-sensing-derived soil moisture products are compared against the results from a deterministic land surface model. The model enables to relate the year 2003 anomalies to a long-term (30 years) climatology. The year 2003 remote sensing derived soil moisture dynamics is compared against a multiyear climatology. The results reveal a negative surface soil moisture anomaly in 2003. The results indicate that there was in general potential to monitor the spatial and temporal dimensions of the low surface soil water content early in 2003 using remote sensing techniques. Both remote sensing data sets indicate a consistent soil moisture decrease in early 2003. A good agreement between the observed surface soil moisture and soil moisture simulations from a land surface process model was found. An outlook to the use of remote-sensing-based soil moisture estimates for large-scale monitoring of surface soil moisture trends is given.

Citation: Loew, A., T. Holmes, and R. de Jeu (2009), The European heat wave 2003: Early indicators from multisensoral microwave remote sensing?, *J. Geophys. Res.*, *114*, D05103, doi:10.1029/2008JD010533.

1. Introduction

[2] The European heat wave of the summer 2003 was an extreme climate anomaly that affected large parts of the European continent. The mean summertime temperatures exceeded the 1961–1990 average by about 3°C to 5°C regionally which corresponds to 5 standard deviations [*Schär et al.*, 2004]. During the first heat wave in May 2003, temperatures raised up to 30°C in Central and Southern Europe [*Ferranti and Viterbo*, 2006]. It was very likely the hottest summer over the past 500 years [*Luterbacher et al.*, 2004].

[3] The socioeconomic impact was disastrous. An excess above the mean mortality rate was observed across Europe, resulting in an increase of the mortality by 70 000 heat related deaths [*MunichRe*, 2008]. Forest fires in Portugal resulted in an economic loss of US$ 1.6 billion [*Heck et al.*, 2004] and the severe drought resulted in uninsured crop losses in Europe totaling about US$ 12.3 billion [*Schär and Jendritzky*, 2004]. Alone in France the official statistics estimated a decrease of crop yield in the order of 15%–28% [*Zaitchik et al.*, 2006].

[4] It is expected that the frequency of severe droughts will increase as a result of Global Climate Change [*Schär et al.*, 2004; *Meehl and Tebaldi*, 2004]. The monitoring and prediction of drought events might therefore become more important. The boundary conditions of heat wave formation have therefore been intensively investigated [*Cassou et al.*, 2005; *Vautard*, 2007]. The year 2003 heat wave was characterized by a long persistent anticyclonic situation with anomalous clear skies and excessive downward net

[1] Max-Planck-Institute for Meteorology, The Land in the Earth System, Hamburg, Germany.
[2] Faculty of Earth and Life Sciences, Department of Hydrology and Geo-environmental Sciences, Vrije Universiteit Amsterdam, Amsterdam, Netherlands.

0148-0227/09/2008JD010533

surface radiative flux. Together with a preceding precipitation deficit in the spring, the radiative forcing contributed to strong evaporation and surface dryout. Several authors suggested that the dry land surface might have contributed to enhance the local heating [*Schär et al.*, 2004; *Black et al.*, 2004].

[5] The evolution of the year 2003 heat wave has been simulated using Regional Climate Models (RCM) [*Ferranti and Viterbo*, 2006; *Fischer et al.*, 2007]. It was found, that the remarkable positive temperature anomalies, which resulted from an anomalous increase of sensible heat flux, are highly likely to be amplified by the spring soil water deficit, although it was not the cause of the event. An early spring onset and anomalous low precipitation in the beginning of the year lasted in a low-root zone soil moisture content and thus a reduced latent heat and increasing sensible heat flux.

[6] *Fischer et al.* [2007] analyzed the effect of initial soil moisture conditions on the forecast skills of a RCM. They found that the RCM was only capable to best reproduce measured temperature anomalies, when the initial soil water content was reduced at the time of the forecast (1st of April). It was shown that the spring root zone soil water content was a very critical parameter to best predict the heat wave evolution. In other words, the RCM model did overestimate the root zone soil water content when not corrected for the spring soil moisture deficit. This resulted in an overestimation of the latent heat and an underestimation of the sensible heat flux. A strong sensitivity of the land surface-atmosphere coupling on initial soil moisture conditions was also found by *Ferranti and Viterbo* [2006]. Thus the initial soil moisture deficit in 2003 seemed to have amplified the evolution of the heat wave and resulted in a further increase of temperature anomalies.

[7] An appropriate characterization of initial land surface conditions is crucial to obtain a good model forecast [*Fischer et al.*, 2007]. As the space-time structure of soil moisture is characterized by a high variability which is the result of complex interactions between terrain characteristics (e.g., topography, land cover, soil), meteorological boundary conditions (e.g., local precipitation, radiation) and land surface processes (e.g., evapotranspiration, lateral soil water fluxes), a prediction of soil water content might be associated with a high degree of uncertainty.

[8] An appropriate monitoring of soil moisture conditions might therefore help to characterize the uncertainties associated with the representation of the soil water content.

[9] Microwave remote sensing techniques provide in general a good opportunity for the monitoring of soil moisture conditions [*Wagner et al.*, 2007b]. The microwave response from natural vegetated and bare soil surfaces has been studied and it has been shown that the microwave emission or backscatter are mainly a function of surface roughness and the moisture content of the surface in case of bare soil conditions [e.g., *Le Hégarat-Mascle et al.*, 2002; *Zribi and Dechambre*, 2002; *Bindlish and Barros*, 2000; *Wigneron et al.*, 2003, 2004]. The presence of vegetation cover can have a considerable influence on the signature, depending on the scattering and attenuation properties of the canopy which are related to vegetation structure and water content [e.g., *Picard et al.*, 2003; *Cookmartin et al.*, 2000; *Loew et al.*, 2006; *Sch t al.*, 2005; *Guglielmetti et al.*, 2008]. However, applications of soil moisture retrievals from existing satellites are hampered as the microwave signal origins only from the uppermost soil layer (0 . . . 5 cm). It has been shown that, given frequent surface soil moisture observations, the estimation of the root zone soil water content can be improved by assimilating the skin soil moisture information into deterministic land surface process models (LSM) [*Walker et al.*, 2001; *Enthekabi et al.*, 1994; *Calvet and Noilhan*, 2000; *Reichle et al.*, 2007].

[10] The present paper investigates whether remote-sensing-based surface soil moisture observations might have been used as an early indicator for the spring 2003 soil water deficit. Two satellite based soil moisture products are used and compared against simulations of a physically based land surface process model. Investigations are made within the mesoscale catchment of the Upper Danube, situated in Southern Germany. The test site was chosen, as it provides a good database for the analysis of the present study. The land surface model (LSM) simulations are used to compare the year 2003 water balance against a 30-year long-term average.

[11] The paper is structured as follows. The remote sensing data and land surface model used are introduced in section 2. The water balance of the year 2003 is investigated and contrasted against a long-term average in section 3. Remote sensing observations are analyzed and compared against the land surface model simulations in section 4. Results are being discussed in section 5. An outlook for continental-scale measurements is given in section 6. Results are summarized and conclusions are drawn in section 7.

2. Data and Models

2.1. Test Site

[12] The Upper Danube catchment, situated in Southern Germany, is used as test site for the present study (Figure 1). The catchment is characterized by large natural gradients. Elevation ranges between 300 and 4 000 m.a.s.l. Yearly precipitation P_a ranges from $500 < P_a < 2500$ mm. Detailed information about land cover, soil texture, elevation and hydrological and meteorological variables is available as part of the GLOWA Danube initiative (www.glowa-danube.de [*Ludwig and Mauser*, 2000]). Land cover information is available from a 30 m land cover map, derived from a fuzzy-logic classification of optical remote sensing data [*Stolz et al.*, 2005]. This high-resolution land cover information was aggregated on a 1 km grid and the fractions for each land cover were estimated for each grid cell. The catchment is dominated by cropland (26%) in the North and grassland areas (14%) in the Southern part close to the mountains of the Alps. Forests are distributed all over the test site with a fraction of 11%.

2.2. Land Surface Model PROMET

[13] The available net radiation R_n [W m^{-2}], which is the sum of the short- and longwave radiation balance, is partitioned into the ground heat flux G, latent heat flux LE and sensible heat flux H

$$R_n = G + LE + H \quad \left[\mathrm{Wm}^{-2}\right] \tag{1}$$

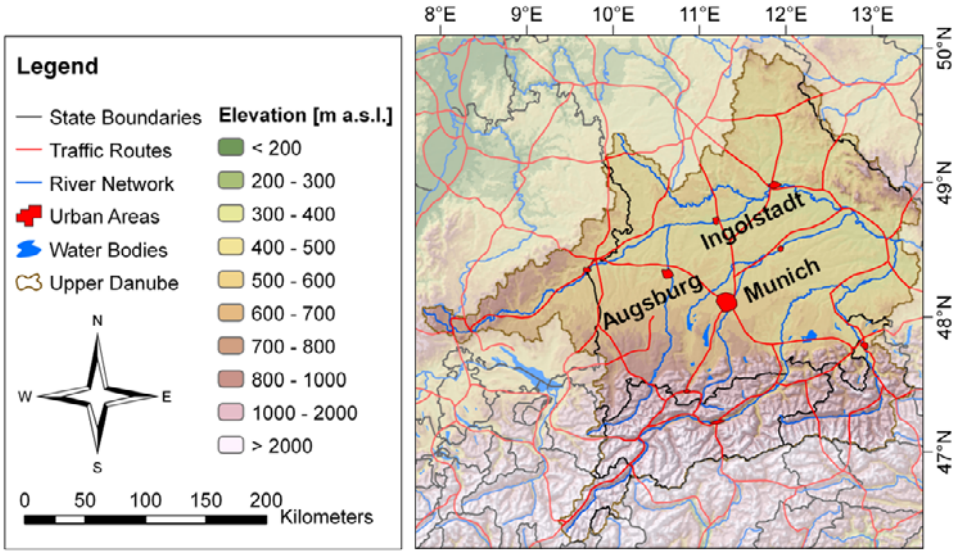

Figure 1. Upper Danube catchment: location and elevation.

[14] A decrease of the latent heat flux *LE* will therefore automatically result in an increase of the sensible heat flux if R_n and G remain constant. The physically based land surface model PROMET (Process Oriented Multiscale EvapoTranspiration model) is used in the present study to simulate the surface energy budget and exchange of water and matter within the soil-plant-atmosphere continuum. The model describes the actual evapotranspiration and water balance at different scales, ranging from point scale, to microscale and mesoscale [*Mauser and Schädlich*, 1998] (W. Mauser and H. Bach, PROMET—A physical hydrological model to study the impact of climate change on the water flows of medium sized mountain watersheds, submitted to *Journal of Hydrology*, 2009, hereinafter referred to as Mauser and Bach, submitted manuscript, 2009). The model consists of a kernel model which is based on five submodules (radiation balance, soil model, vegetation model, aerodynamic model, snow model) to simulate the actual water and energy fluxes and a spatial data modeller, which provides and organizes the spatial input data on the field-, micro- and macroscale. The simulations are made on hourly basis.

[15] PROMET solves the surface energy balance in an iterative way. The ground heat flux is estimated using a soil temperature model [*Muerth*, 2008]. Actual evapotranspiration is simulated within PROMET using the Penman-Monteith equation [*Monteith*, 1965]. Canopy surface resistance is simulated as a function of vegetation type using a resistance network approach [*Baldocchi et al.*, 1987], while the soil resistance is estimated on the basis of the approach of *Eagleson* [1978]. A four-layer soil model (0–5, 5–20, 20–65, 65–200 cm) is used to calculate soil water fluxes and soil temperature profiles. The change of volumetric soil moisture content, percolation, exfiltration, capillary rise and surface runoff are explicitly considered. The infiltration into the soil layer is described using the model of *Philip* [1957]. The soil water retention model of *Brooks and Corey* [1964] is used to relate soil moisture content to soil suction head. A detailed description of the model is given by *Mauser and Schädlich* [1998] and Mauser and Bach (submitted manuscript, 2009). The soil water model has been validated in different test sites using in-situ soil moisture measurements of soil moisture profiles [*Pauwels et al.*, 2008]. A physical snow model extends PROMET to allow for simulations in cold climates [*Strasser and Mauser*, 2001].

[16] PROMET simulations are based on GIS information as, e.g., soil maps and land use information. Meteorological forcing data might be either provided from station networks as well as from gridded forcing fields. PROMET has been extensively validated in different geographic locations in Central Europe (Upper Rhine Valley: 10×10 km^2, Bavarian Alpine Foreland: 200×100 km^2, Upper Danube catchment: 76,000 km^2, Weser catchment: 35,000 km^2) using evapotranspiration measurements of micrometeorological stations at the local scale and by comparison with thermal remote sensing information at the regional scale [*Mauser and Schädlich*, 1998; *Ludwig and Mauser*, 2000].

[17] It provides interfaces to integrate remote-sensing-derived information into the model. It has been used together with optical and microwave remote sensing data to improve land surface simulations. *Bach and Mauser* [2003] used the model to improve crop yield prediction and surface runoff prediction by combining PROMET results with optical (Landsat-TM) and microwave (ERS) remote sensing data. *Schneider* [2003] used LANDSAT-TM data to determine vegetation model parameters and improve plant growth simulations. *Loew et al.* [2007] compared PROMET simulations at different spatial scales with soil moisture information derived from active microwave data [*Loew et al.*, 2006], and found a good agreement between the spatial patterns of observed and simulated soil moisture at multiple scales.

2.3. Remote Sensing Data

[18] The remote sensing data used in the present study are based on observations from two complementary satellite sensors. The data from an active microwave instrument with high spatial resolution, but low temporal frequency is contrasted against observations from a sensor with medium

Table 1. ENVISAT ASAR Scenes

Date	Acquisition Time	Mode	Polarization	Track
4 Mar 2003	21:01	Ascending	VV	215
20 Mar 2003	09:37	Descending	VV	437
5 Apr 2003	09:34	Descending	VV	165
10 May 2003	09:34	Descending	VV	165

spatial resolutions but high temporal frequency. The intercomparison of both data sets allows for the evaluation of the trade-off in using sensors with reduced spatial resolutions for monitoring trends in surface soil moisture over larger areas.

2.3.1. ENVISAT ASAR Data

[19] The European ENVISAT satellite with its Advanced Synthetic Aperture Radar (ASAR) is an active microwave sensor, operating at C-band (5.3 GHz) [*ESA*, 2002]. It provides multiple acquisition modes which allow for the coverage of an area of interest at different imaging geometries. The medium resolution Wide Swath Mode (WSM) with a spatial resolution of approximately 150 m is used in the present investigation. The WSM mode allows for a wide area coverage (swath width: 400 km) to give a synoptic overview about the land surface conditions of a larger area (e.g., a mesoscale hydrological catchment). Four image data sets were acquired over the test area within the period from the beginning of March to the mid of May 2003. Table 1 lists the characteristics of the data sets used in the present study.

[20] An appropriate preprocessing of the image data is required to enable the retrieval of quantitative information from the remote sensing data. The image data is therefore geometrically and radiometrically corrected using a digital elevation model (DEM) [*Loew and Mauser*, 2007].

[21] Soil moisture products are then derived from the such obtained normalized microwave backscattering coefficient σ^0 following the procedure described in *Loew et al.* [2006]. The method is based on the decomposition of the microwave signal into components with and without soil moisture information using a priori land cover information. The backscattering coefficient is then corrected for contributions from areas without sensitivity to surface soil moisture (e.g., forested or urban areas) and finally the soil dielectric properties are estimated from the remaining backscattering signal by inversion of a semiempirical backscattering model. The such derived soil dielectric characteristics are then used to calculate soil water content θ using a priori information on soil texture (sand, clay content) and a dielectric mixing model [*Dobson et al.*, 1985]. The algorithm has been validated in numerous studies [*Bach and Mauser*, 2003; *Loew et al.*, 2006] and it was found that the accuracy of the soil moisture estimates is between 3 and 7 vol.% [m^3 m^{-3}] rms error.

2.3.2. AMSR-E

[22] The Advanced Microwave Scanning Radiometer (AMSR-E) is a passive microwave scanning radiometer, operating at six different wavelengths within the microwave spectrum (6.925, 10.65, 18.7, 23.8, 36.5, and 89GHz). The sensor measures the microwave brightness temperature T_b^p at horizontal and vertical polarizations (p = h, v). The large area coverage (swath width: 1445 km) allows for a frequent coverage of the globe in the order of three days with increasing frequencies a er latitudes. The spatial resolution of the different channels is varying from 5 km (89 GHz) to 56 km (6.925 GHz) [*Njoku et al.*, 2003].

[23] A globally available soil moisture data set, provided by the VU University Amsterdam together with NASA Goddard Space Flight Centre, is used in the present study [*Owe et al.*, 2008]. The soil moisture retrievals are based on the solution of a microwave radiative transfer model and solve simultaneously for the surface soil moisture and vegetation optical depth without a priori information of land surface characteristics [*Meesters et al.*, 2005]. The flexible approach allows in general for the retrieval of soil moisture from a variety of frequencies. The C-band (6.925 GHz) data product is used in the present study as it was found to have a higher sensitivity to surface soil moisture dynamics. The soil moisture C-band products have been validated over a large range of study areas with high correlations with in situ observations in semi arid regions (r = 0.79, RMSE = 0.03 [m^3 m^{-3}] for the Murrumbidgee Soil Moisture Monitoring Network in Australia [*Draper et al.*, 2007]; r = 0.83, RMSE = 0.06 [m^3 m^{-3}] for the REMEDHUS soil moisture network in Spain [*Wagner et al.*, 2007b]) and somewhat lower in agricultural areas (r = 0.78, RMSE = 0.2 [m^3 m^{-3}] for the SMOSREX site in France [*Rüdiger et al.*, 2009]. The data set is now public available (http://www.geo.vu.nl/jeur/lprm) and will be available through a user friendly web map server by the end of 2008 (http://adaguc.knmi.nl). The ascending and descending modes in general show a good soil moisture retrieval performance over Europe. However, based on our analysis, the daytime ascending pass data appeared less noisy and was therefore chosen for this study.

3. Water Balance Within the Upper Danube 2003

[24] The year 2003 anomalies within the Upper Danube test site are investigated in the following section. First, the meteorological conditions are compared against a 30-year reference period (1971–2000). Further, PROMET model simulations are used to quantify the impact of the year 2003 heat wave on the water balance within the Upper Danube catchment. The model simulations are based on measured meteorological forcing data from a dense network of stations from the German Weather Service (DWD). A total of 220 stations are situated within the catchment, resulting in an average station density in the order of 20 km. The resolution of the model is 1 × 1 km^2.

[25] Figure 2 shows the temperature anomalies in the year 2003 within the catchment as observed from meteorological records. Maximal monthly mean temperatures are observed in August with values greater than 20°C. This corresponds to positive temperature anomalies, compared to the 30 year average, from February to September with a maximum monthly mean anomaly of 5.5°C in June 2003.

[26] Except from January, the year was characterized by a pronounced reduction of precipitation throughout the year. It can be expected that the precipitation deficit would result in a soil water deficit within the catchment. To quantify the impact of the anomalous low precipitation and high temperatures on the water budget, the PROMET model is used to calculate the water and energy fluxes for the year 2003 and compare these model simulations against the 30 year average. The model is forced using interpolated station data from meteorological stations of the German Weather Ser-

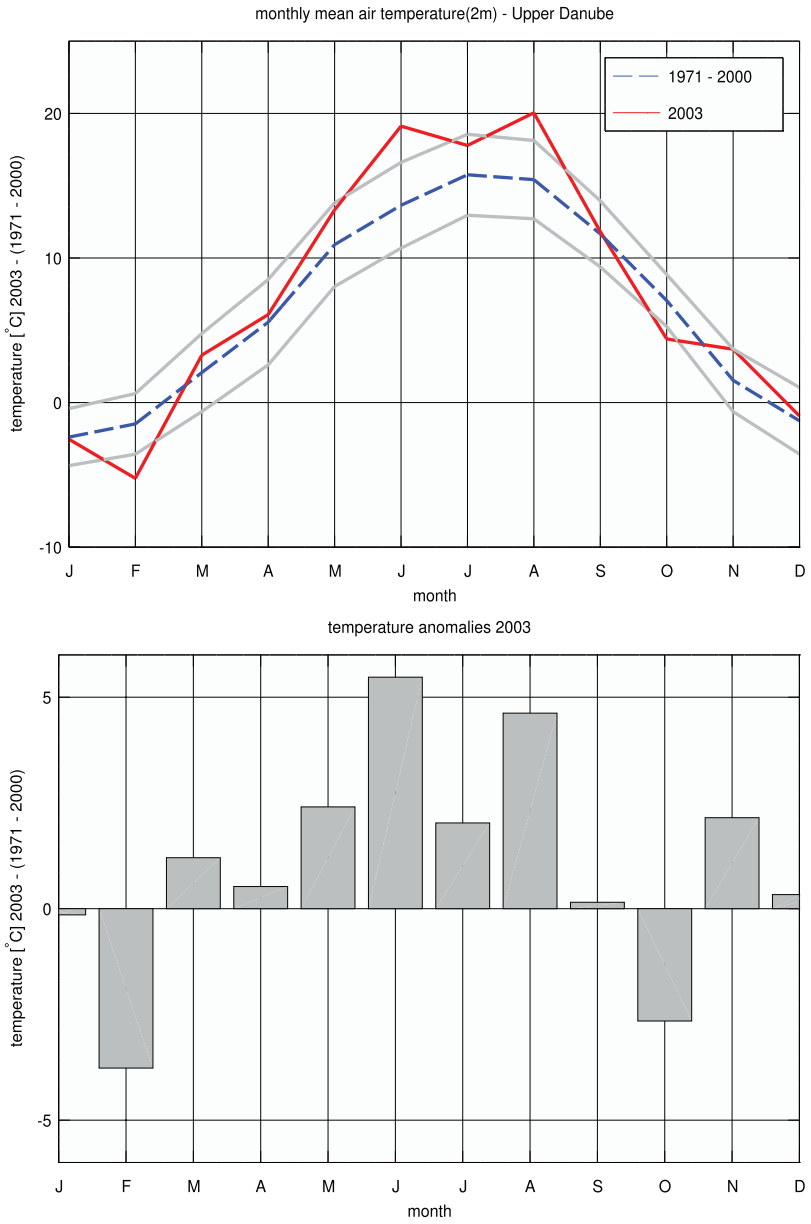

Figure 2. Air temperature (2 m) of the year 2003 against the (left) long-term average and temperature anomalies for the (right) individual months in the Upper Danube; grey lines indicate 1σ.

vice (DWD) [*Mauser and Schädlich*, 1998]. Mauser and Bach (submitted manuscript, 2009) have investigated the model performance throughout this 30 year reference period and found good agreement of the model simulated water budget with observational data.

[27] Figure 3 shows the year 2003 surface and root zone (2 m) soil water content for various land cover types as simulated by PROMET. Surface soil moisture is denoted as θ_s, while root zone soil moisture is denoted as θ_r in the following. The long-term average and its 1σ confidence interval are derived from a 30-year model climatology for the particular grid cell of the model. A pronounced low soil water content is observed in the year 2003 for all three land cover types. A deficit in the root zone soil water content is already recognized early in the year (April, May) with a much steeper decrease of the soil moisture than under normal summer conditions. Maximum deviations from the long-term mean are observed with deviations greater than 2σ in July, August and September for the deciduous forest and in August and September for the wheat respectively. The larger deficit for the forest results from a stronger evapotranspiration loss.

[28] A linkage between θ_s and θ_r can only be achieved by modelling of the soil water fluxes throughout the temporal integration of the land surface model. As one would expect, the temporal variability of θ_s is much higher than for θ_r. However, also θ_s shows a pronounced anomaly in the year 2003 for all three land cover classes. Especially in the spring period (March to May), θ_s is much lower than the long-term average and the deviation exceeds 1σ from mid of March to May. Although the short-term variability of θ_s is driven by precipitation events, the very low soil moisture

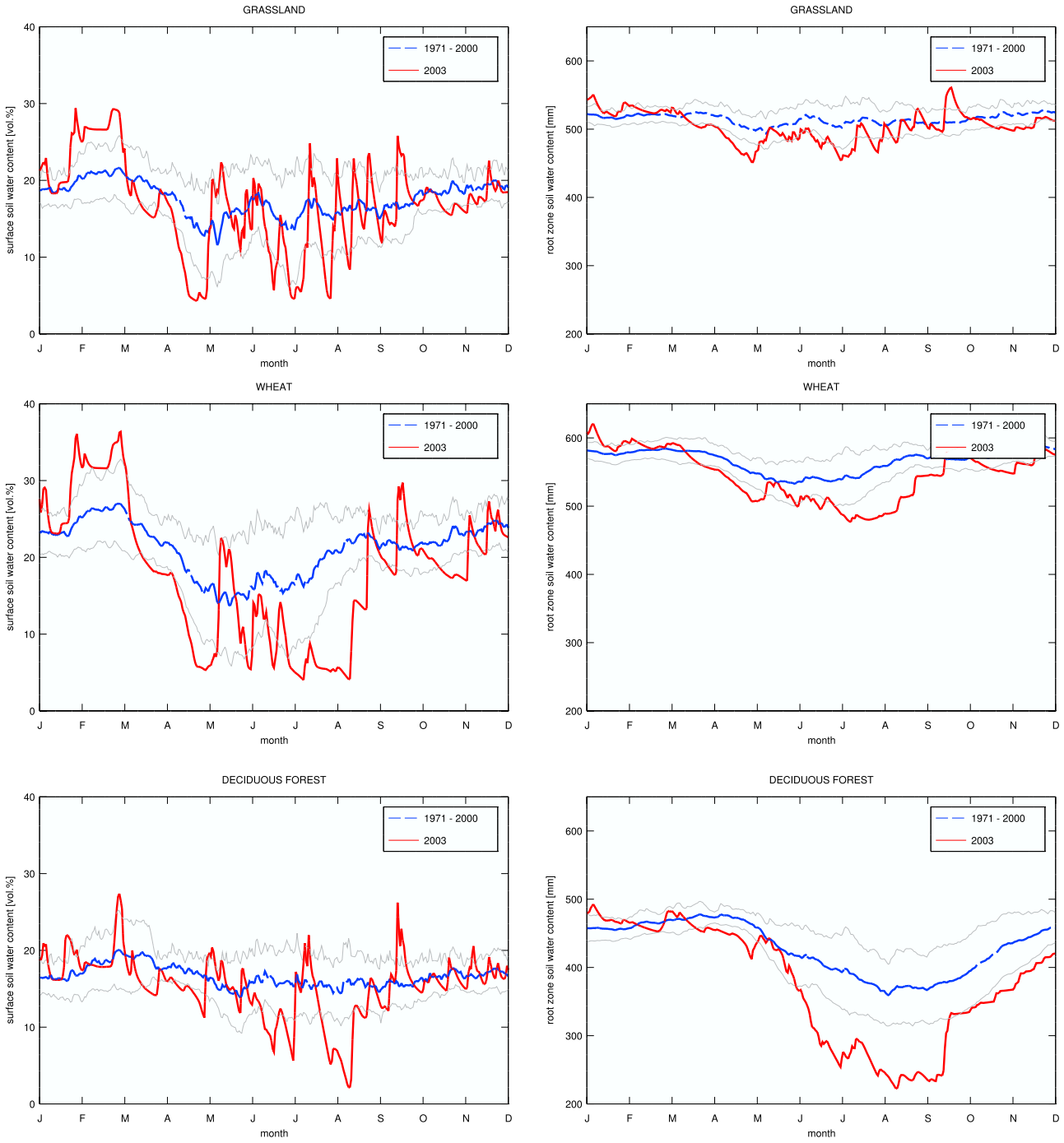

Figure 3. (left) Simulated surface and (right) root zone daily soil water content for the year 2003 compared to the long-term average (1971–2000) for three different land cover types in the Upper Danube: (top) grassland, (middle) wheat, (bottom) forest. The grey lines represent 1σ of the 30-year period.

conditions in the summer months (JJA) are also observed in the simulations for θ_s. This indicates a similar course in the overall trends of θ_s and θ_r, so θ_s might provide a suitable proxy for the long-term course of the soil water content, especially in spring 2003.

4. Data Analysis

[29] It will be investigated in the following, whether the low surface soil moist nditions in spring 2003 were observable by means of microwave remote sensing data. Surface soil moisture maps were generated from all data sets and are compared in the following.

4.1. ENVISAT ASAR Data

[30] The soil moisture maps produced from ENVISAT ASAR data are shown in Figure 4. These data sets have a 1×1 km^2 spatial resolution and are projected to an equal area Lambert conical projection [*Bugayevskiy and Snyder*, 1995]. Forested and urban areas as well as open water

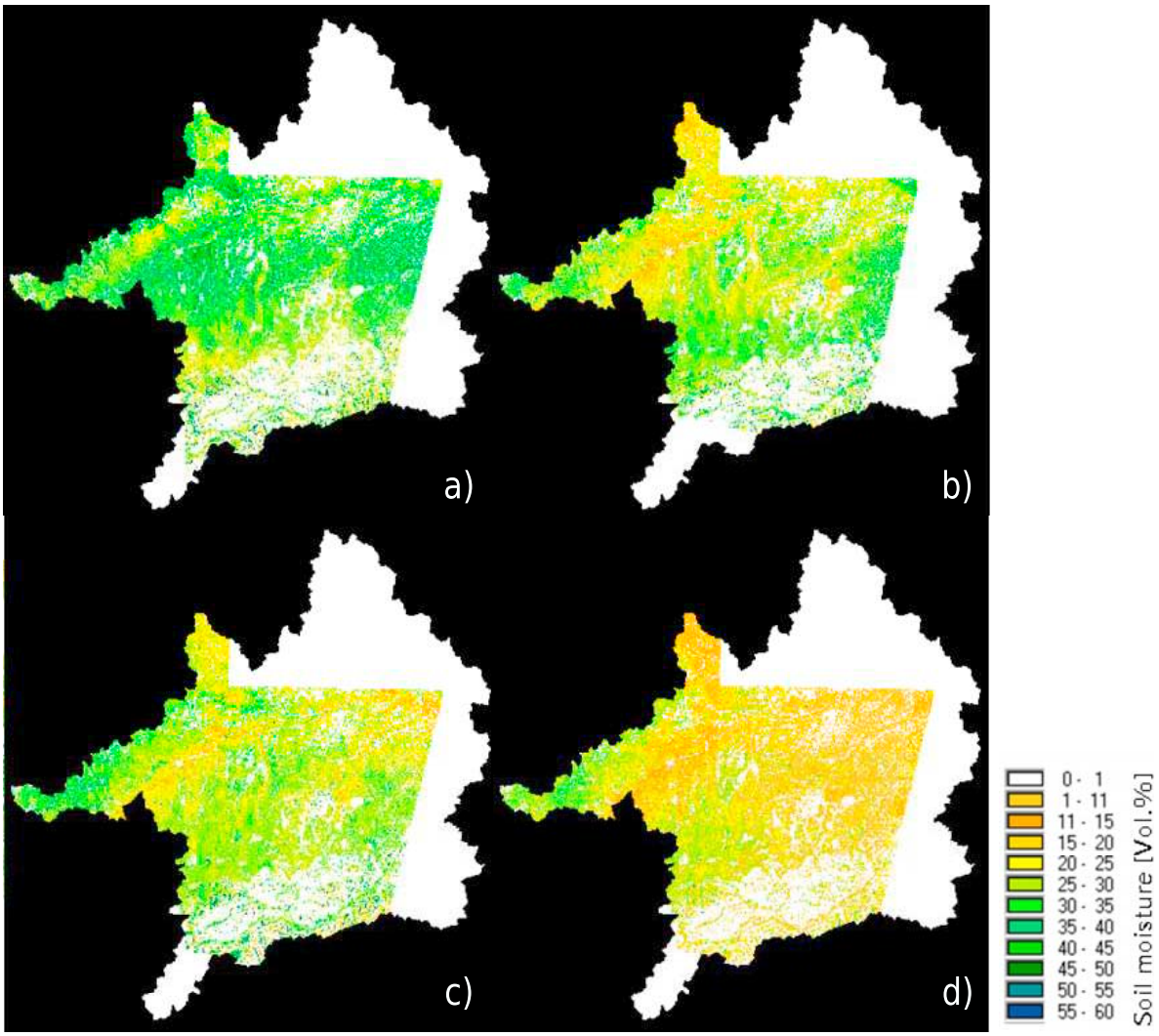

Figure 4. Surface soil moisture maps from ENVISAT ASAR in spring 2003: (a) 04.03, (b) 20.03, (c) 05.04, (d) 10.05.

bodies are masked in the remote sensing product as the microwave signal is not sensitive to soil moisture changes in those areas.

[31] The remote sensing products show a considerable decrease of the surface soil moisture content. The spatially averaged surface soil water content and its standard deviation was determined as 32.8 ± 6.4, 25.4 ± 6.9, 27.3 ± 6.7 and 17.9 ± 9.2 vol.% [m^3 m^{-3}] for the 4 March 2003, 20 March 2003, 5 April 2003 and 10 May 2003 respectively which corresponds to a decline of 0.2 vol.% per day in the average.

4.2. AMSR-E Data

[32] The analysis of the AMSR-E soil moisture product revealed strong temporal variations and the signal was found to be noisy. Part of this noise is explained by a varying location of the center of the sensors footprint relative to a stable reference point. It was also found that the soil moisture retrievals contained considerable high values, which are considered as a positive bias. There are various reasons that could result in biased soil moisture estimates from origina SR-E brightness temperature records. Subpixel land cover fractions might, e.g., introduce a bias in the soil moisture retrievals from a passive microwave system [*Loew*, 2008]. In addition, uncertainties in soil texture as well as topographic effects might result in biased retrieval results. The data was therefore filtered using a moving average filter with a filter window of 7 days before the data analysis. The filtering considerably reduced the high-frequency soil moisture changes and the such obtained soil moisture time series was used in the further analysis. A sensitivity analysis of the impact of the filtering procedure on the estimate of the temporal trends in spring 2003 soil moisture revealed, that the filtering procedure did not influence the obtained results, shown in the following section. The data was normalized by subtracting the average soil moisture value, estimated from the entire year 2003.

4.3. Intercomparison

[33] To perform a cross comparison between the different data sets, these are reprojected to a common, equal area grid. The Icosahedral Snyder Equal Area projection (ISEA) was used as the reference projection [*Sahr et al.*, 2003]. The ISEA grid used (ISEA4H9) has a spacing in the order

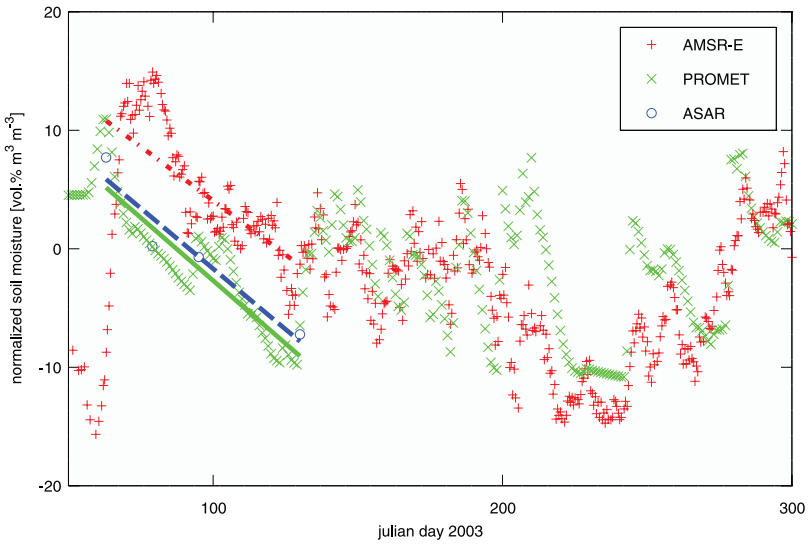

Figure 5. Example of surface soil moisture evolution for an ISEA grid cell as estimated from all three data sets.

of 20 km. The same projection is also used as reference for the forthcoming SMOS mission. The reprojection of the data was achieved by assigning all pixels of the soil moisture maps to the closest ISEA grid point. In case that more than one soil moisture value was assigned to an ISEA grid point, the arithmetic average was calculated.

[34] A direct comparison between the different data sets is hampered by the fact that each soil moisture product has it's own climatology and biases. However, the relative soil moisture changes are assumed to be consistent within each data set. To enable a better inter comparison of the relative changes of soil moisture as observed from the individual soil moisture data sets, the data was normalized by subtracting the mean value of the entire available time series.

[35] It is investigated in the following on basis of the ISEA grid, whether the different data sets show a similar soil moisture dynamics in spring 2003.

[36] The analysis is focused on the period from Julian Day (JD) 63 to JD 130 which corresponds to the period where all data sets were available. Figure 5 shows an example of the soil moisture evolution from the three different sources for an ISEA grid node. A similar decrease in the soil water content is observed. A linear regression is calculated for the spring 2003 period (JD 63 – JD 130). The gain m is -0.20, -0.18 and -0.21 for the ENVISAT ASAR, AMSR-E and PROMET surface soil moisture data respectively. While the ENVISAT ASAR observations were only available for the year 2003 for the present study, the AMSR-E data only allows for an interannual comparison. The remote sensing time series for the years 2004, 2005 and 2006 were processed similar to the year 2003 data set to evaluate whether the observed year 2003 soil moisture decline was an anomaly or whether it corresponds to a typical spring soil moisture decrease during the investigation period. The estimated gains m for the same grid node as shown in Figure 5 are 0.03, 0.15 and 0.09 for the years 2004, 2005 and 2006 respectively. A strong decrease (-0.18) of the surface soil moisture is only observed in the year 2003, indicating an anomalous soil moisture dynamics in that year.

[37] Using the available time series for each ISEA grid node, a value for m can be estimated. Figure 6 shows the frequency distribution of m as estimated from all three data sets over the entire test site. All three soil moisture data sets indicate a negative gain in spring 2003 with mean values of $m = -0.19$, -0.22 and -0.18 for ENVISAT ASAR, AMSR-E and PROMET respectively. Negative gains are observed for most parts of the test site. Figure 7 shows maps of m for all three data sets. Coherent spatial patterns of the soil moisture decrease within the test site are observed. The spatial pattern of m is organized and not random. In addition, all three data sets show the strongest decrease in surface soil water content in the eastern part of the test site with $m < -0.35$. Especially the satellite data shows a strong decline in these areas which are dominated by arable land. Cropland areas are expected to have highest sensitivity of the microwave signal to surface soil moisture dynamics, whereas urban or forested regions have lower sensitivity [*Loew*, 2008].

[38] However, the alpine areas show distinct differences in the response of the soil moisture signal. While the AMSR-E products seem to indicate a strong increase of the soil water content, PROMET simulations were found to be indifferent ($m \approx 0$) and the ASAR data shows a decrease. Alpine areas are known to highly affect the microwave signal of active as well as passive microwave sensors [*Mätzler and Standley*, 2000; *Loew and Mauser*, 2007]. It is therefore expected that no reliable information on the surface characteristics can be extracted from the remote sensing products in those areas.

[39] Figure 8 shows a scatterplot of the gain m on basis of the individual ISEA grid nodes.

[40] Alpine areas are shown in blue and nonalpine grid nodes are in red. The intercomparison between the three data sets for the nonalpine regions shows that a similar surface soil moisture decline is observed for all three data sets. The values for m are much closer to the 1:1 line in those cases. Rather different values for m were observed for areas with large terrain slopes. The AMSR-E data tends to

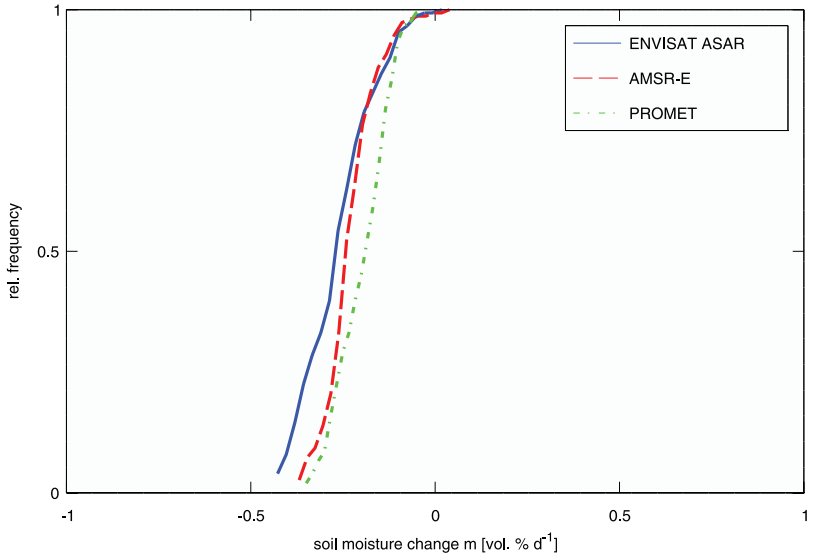

Figure 6. Frequency distribution of surface soil moisture decrease m as estimated from satellite and LSM soil moisture climatologies for the Upper Danube catchment.

overestimate m in the alpine regions, compared to the other data sets.

5. Discussion

[41] It has been shown that the three completely independent surface soil moisture data sets show consistent surface soil moisture dynamics within the Upper Danube test site in spring 2003. PROMET surface soil moisture simulations as well as satellite based estimates show a consistent decline of surface soil moisture in the order of 0.2 vol.% per day. Despite the fact that the used soil moisture data sets are very different in terms of spatial and temporal coverage and that they represent only a thin surface soil layer, it is promising that consistent spatial patterns could be observed for the limited reference period used for the present study. The analysis on basis of individual grid nodes also revealed good correlations between the data sets for nonalpine regions.

[42] PROMET land surface model simulations indicate that the observed soil moisture deficit in spring 2003 is significantly different from the long-term average, both for surface as well as root zone soil water content.

[43] The results outline in general the potential of using satellite data for the monitoring of surface soil moisture dynamics at larger spatial scales. The Upper Danube catchment provided an ideal framework for the intercomparison of the different data sets, as the remote sensing data as well as model simulations were available for the cross comparison.

[44] However, an application to larger spatial scales and longer time series would be needed to evaluate the robustness and transferability of the obtained results.

6. Continental-Scale Application

[45] The PROMET model simulations as well as the ENVISAT ASAR data are restricted to the Upper Danube catchment in the present study. In general it would be possible to apply the L well as the derivation of soil moisture from ASAR at a much wider spatial extent. However, this requires the availability of appropriate forcing data for the model simulations and a consistent large spatial coverage of the ASAR data. Both limit the analysis of the present study to the Upper Danube test area.

[46] However, the AMSR-E data is available with high temporal resolution at global scale. In addition, the used data product will be available in near real time mode by end of 2008 throughout a user friendly web interface, which allows the online monitoring of surface soil moisture dynamics. The potential of using the AMSR-E data to monitor the decline of surface soil moisture in spring 2003 at continental scale was therefore evaluated. Figure 9 shows the estimated gain of the soil moisture change m as derived from AMSR-E over Europe. A considerable decrease of soil moisture is observed for most areas. For 50% of the area the gain is $m < -0.2$, while a negative gain is observed for 80% of the continent. The estimated soil moisture decrease shows coherent spatial patterns. The strongest decrease is observed in the southeastern part of France, where the center of the summer heat wave occurred, while more northern parts of the continent show a lower surface soil moisture decline.

[47] A considerable effect of topography on the observed soil moisture dynamics is recognized. Areas like the Alps, show indifferent or positive values for m. An appropriate masking of those areas therefore seems to be needed before further analysis. This can be achieved by using, e.g., topographic indices [*Mialon et al.*, 2008]. In addition, highly forested areas with no soil moisture sensitivity can be discarded from an analysis by masking areas with a high optical thickness. This ancillary information is provided together with the AMSR-E data product.

[48] The year 2003 surface soil moisture decrease was compared against the average soil moisture dynamics of the years 2003 to 2006. For each year, m was calculated similar to the year 2003 and the average of the four years was estimated. Figure 9 shows the anomaly of the year 2003

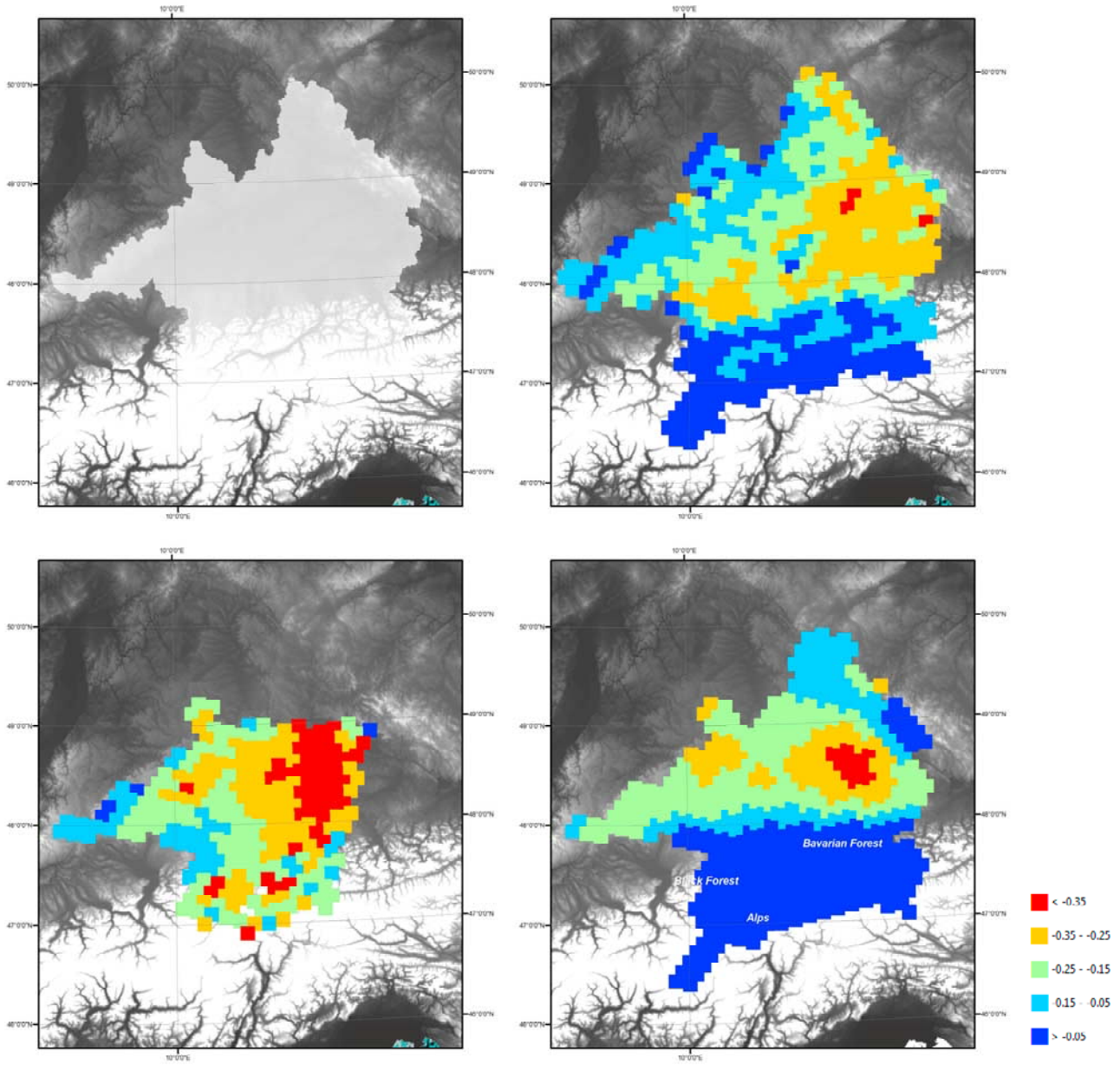

Figure 7. (a) Upper Danube catchment and estimated surface soil moisture decline in spring 2003 as derived from (b) PROMET simulations, (c) ENVISAT ASAR, and (d) AMSR-E.

spring surface soil moisture dynamics and its frequency distribution. Negative anomalies indicate that the decrease of soil moisture was higher in 2003 than in the average. For 90% of the investigated domain, a higher surface soil moisture decrease was observed in 2003. The pattern of the anomaly shows clearly an anomalous high soil moisture decrease in the area of southeastern France, the Rhone valley and parts of Southern Germany. The year 2003 surface soil moisture anomaly shows good agreement with the recorded springtime precipitation anomalies, provided by the Global Precipitation Climatology Centre (GPCC) [*Schneider et al.*, 2008]. The remote-sensing-derived information shows strongest decrease of surface soil moisture in the regions, where the largest negative precipitation anomalies occurred, centered heastern France. Also the zone of negative precipitation anomalies in the Northern part of Spain as well as in Northern England can be recognized.

7. Conclusion

[49] It has been shown that remote sensing techniques could be used to monitor the decline of surface soil water content, within the Upper Danube catchment, in spring 2003 using microwave sensors. Agreement of the remote-sensing-derived soil moisture dynamics with the simulations of a state-of-the-art land surface model, were found, which is in general a promising result. However, it is emphasized that the study provides only a first analysis that shows the general consistency of surface soil moisture signals obtained from different remote sensing observations

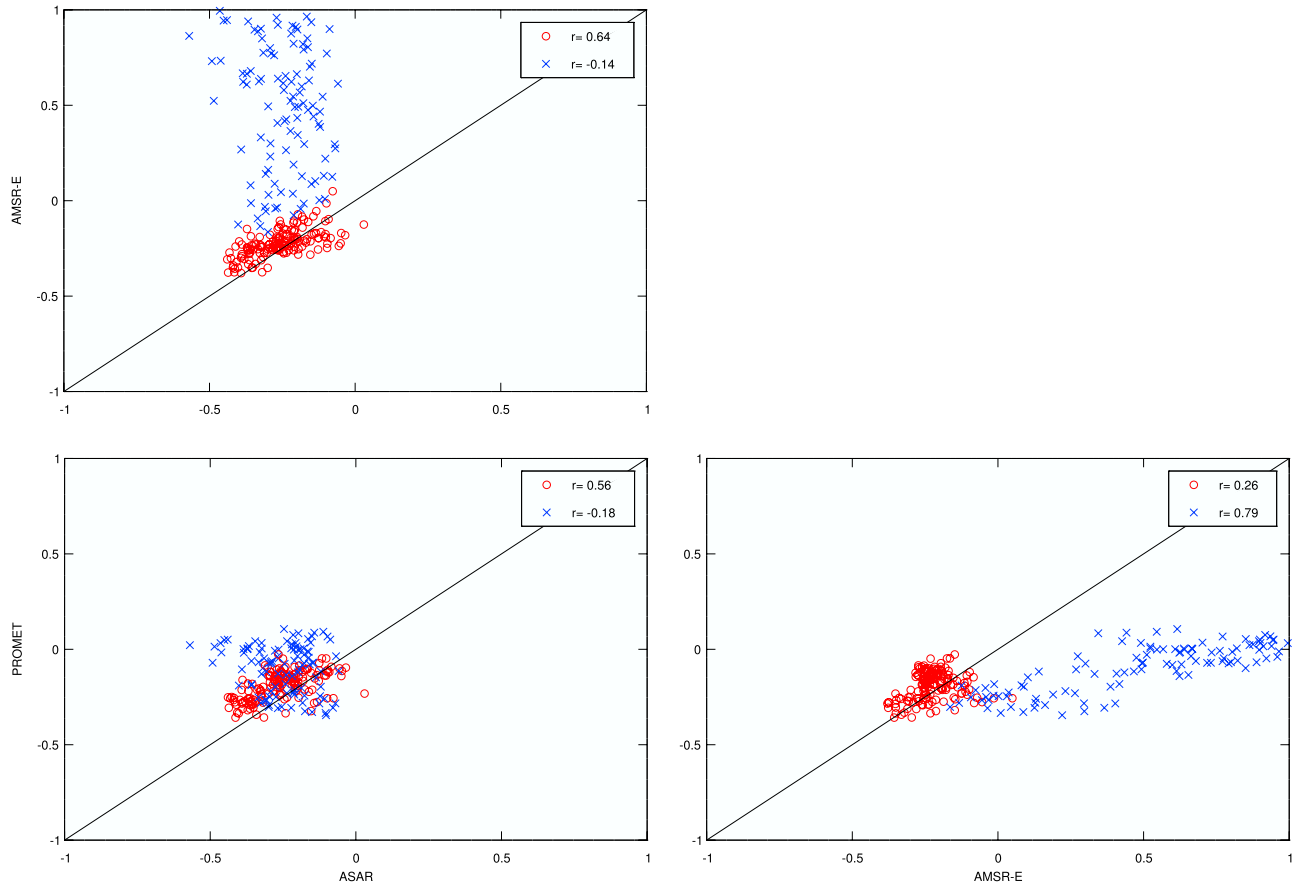

Figure 8. Intercomparison of spring 2003 surface soil moisture change [vol.% day^{-1}] in the Upper Danube catchment as observed from satellite observations and PROMET simulations. Each point represents an ISEA grid node. (crosses) Alpine areas; (circles) nonalpine areas with corresponding correlation coefficients *r*.

and model simulations. Further research is needed to develop robust early warning indicators for low soil water deficits based on satellite observations.

[50] PROMET model simulations are driven by measured climate data from a dense network of stations. However, dense station data is often only available with a time delay of several weeks and restricted to areas where such an infrastructure is available and maintained. The integration of satellite information into land surface process models might be therefore a valuable tool to improve the model simulations skills by either determining necessary model input parameters as, e.g., distributed information on soil characteristics or land cover as well as compensating for deficits in meteorological input data or the model itself by updating the model simulations when observations become available [*Santanello et al.*, 2007; *Loew and Mauser*, 2008b; *Loew et al.*, 2009].

[51] Numerous studies have outlined that there is in general potential to improve simulations of root zone soil moisture by sequentially assimilating surface soil moisture information [*Calvet and Noilhan*, 2000; *Walker et al.*, 2001; *Enthekabi et al.*, 1994; *Reichle et al.*, 2002]. *Reichle et al.* [2007] have investigated the potential to improve the simulations of a global land hydrology model by assimilating surface soil moisture i ation derived from AMSR-E data. They found slight improvements of the model skills, comparing the model simulations against ground observations. New sensor systems like, e.g., the forthcoming Soil Moisture and Ocean Salinity mission (SMOS), to be launched in 2009 [*Kerr et al.*, 2001], are expected to provide data with a higher sensitivity to root zone soil moisture content than the existing satellite systems.

[52] Integrating this information into dynamic regional climate models would probably allow for an improved model initialization and thus to improve their forecasting skills. Frequent observations and wide area coverage might be a prerequisite for that purpose. As the present investigation was limited to a rather small area and a very limited data set, based on active microwave observations, an integration of the remote sensing data into, e.g., RCMs and update of their model state is not reasonable. Using sensors with higher temporal frequency, as microwave radiometers or scatterometers, such an integration would be feasible. However, these sensors have spatial resolutions in the order of tens of kilometers [*Wagner et al.*, 2007a].

[53] To account for the heterogeneity of the land surface at these spatial scales, different kind of approaches have been proposed to disaggregate soil moisture information derived from these coarse resolution data sources. These are based on synergistical use of the coarse resolution data together

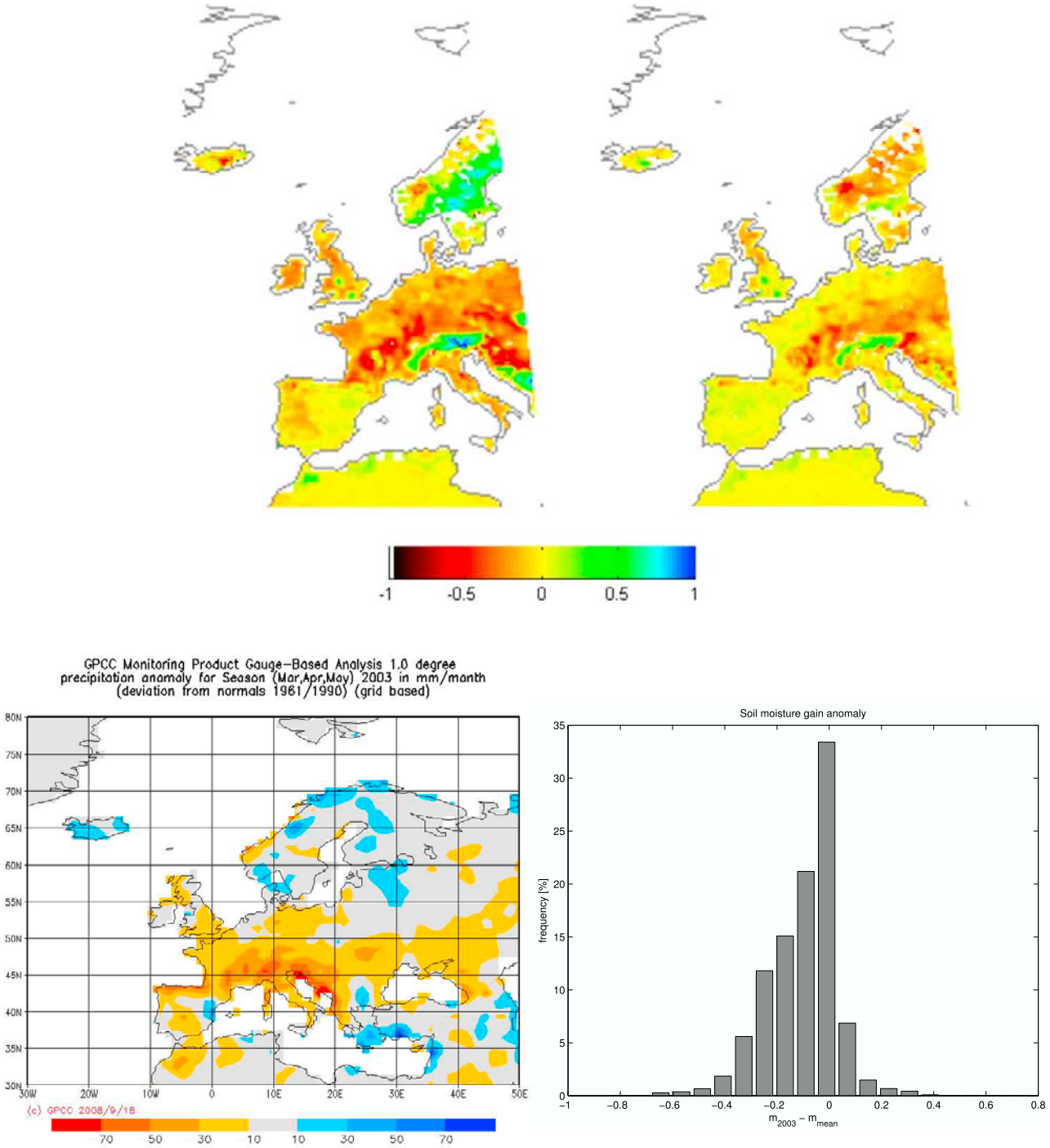

Figure 9. Springtime surface soil moisture decrease (m_{2003}) as observed from (a) AMSR-E in 2003, (b) anomaly plot of m_{2003}, and (d) its frequency distribution. (c) GPCC springtime precipitation anomaly and frequency distribution.

with a priori knowledge of characteristic soil moisture fields [*Wagner et al.*, 2008; *Loew and Mauser*, 2008a].

[54] A synergy of sensors with high and low spatial resolutions might be useful to improve the characterization of land surface conditions at appropriate temporal and spatial scales and thus help to support regional climate modeling applications which might yield to improved medium range forecasting skills and thus, e.g., early warning systems for hydrometeorological extreme events.

[55] **Acknowledgments.** The ENVISAT ASAR data were provided by ESA throughout the PI-program, which is gratefully acknowledged. Meteorological data were kindly provided by the German Weather Service (DWD).

References

Bach, H., and W. Mauser (2003), Methods and examples of for remote sensing data assimilation in land surface process modelling, *IEEE Trans. Geosci. Remote Sens.*, *41*(7), 1629–1637.

Baldocchi, D., B. Hicks, and P. Camara (1987), A canopy stomatal resistance model for gaseous depositions to vegetated surfaces, *Atmos. Environ.*, *21*(1), 91–101.

Bindlish, R., and A. P. Barros (2000), Multifrequency soil moisture inversion from SAR measurements with the use of IEM, *Remote Sens. Environ.*, *71*, 67–88.

Black, E., M. Blackburn, G. Harrison, B. Hoskins, and J. Methven (2004), Factors contributing to the summer 2003 European heatwave, *Weather*, *59*, 217–223.

Brooks, R., and A. Corey (1964), Hydraulic properties of porous media, in *Tech. Rep., Hyd. Pap. 3*, Colo. State Univ., Fort Collins, Colo.

Bugayevskiy, L., and J. Snyder (1995), *Map Projections—A Reference Manual*, Taylor and Francis, Philadelphia, Pa.

Calvet, J., and J. Noilhan (2000), From near surface to root zone soil moisture using year-round data, *J. Hydrometeorol.*, *1*, 393–411.

Cassou, C., L. Terray, and A. Phillips (2005), Tropical Atlantic influence on European heat waves, *J. Clim.*, *18*(15), 2805–2811.

Cookmartin, G., P. Saich, S. Quegan, R. Cordey, P. Burgess-Allen, and A. Sowter (2000), Modeling microwave interaction with crops and comparison with ERS-2 SAR observations, *IEEE Trans. Geosci. Remote Sens.*, *38*(2), 658–670.

Dobson, M., F. Ulaby, M. T. Hallikainen, and M. El Rayes (1985), Microwave dielectric behavior of wet soil. part II: Dielectric mixing models, *IEEE Trans. Geosci. Remote Sens.*, *GE-25*(1), 35–46.

Draper, C., J. Walker, P. Steinle, R. de Jeu, and T. Holmes (2007), Remotely sensed soil moisture over Australia from AMSR-E, in *Proc. MODSIM 2007 International Congress on Modelling and Simulation, Christchurch, New Zealand*, Modelling and Simulation Society of Australia and New Zealand, Lincoln.

Eagleson, P. (1978), Climate, soil, and vegetation, simplified model of soil-moisture movement in liquid-phase, *Water Resour. Res.*, *14*(5), 722–730.

Enthekabi, D., H. Nakamura, and E. Njoku (1994), Solving the inverse problem for soil moisture and temperature profiles by sequential assimilation of multifrequency remotely sensed observations, *IEEE Trans. Geosci. Remote Sens.*, *32*(2), 438–448.

ESA (Ed.) (2002), *EnviSAT ASAR Product Handbook*, Issue 1.1, 1st December, Frascati, Italy.

Ferranti, L., and P. Viterbo (2006), The European summer of 2003: Sensitivity to soil water initial conditions, *J. Clim.*, *19*, 3659–3680.

Fischer, E., S. Seneviratne, P. L. Vidale, D. Lüthi, and C. Schär (2007), Soil moisture atmosphere interactions during the 2003 European summer heat wave, *J. Clim.*, *20*, 5081–5099.

Guglielmetti, M., M. Schwank, C. Mtzler, C. Oberdrster, J. Vanderborght, and H. Flhler (2008), FOSMEX: Forest soil moisture experiments with microwave radiometry, *IEEE Trans. Geosci. Remote Sens.*, *46*(3), 727–735.

Heck, P., A. Zanetti, R. Enz, J. Green, and S. Suter (2004), Natural catastrophes and man-made disasters in 2003, in *Sigma Rep. 1/2004, Swiss Re Tech. Rep.*, pp. 1–10, SwissRe, Zurich.

Kerr, Y. H., P. Waldteufel, J.-P. Wigneron, J.-M. Martinuzzi, J. Font, and M. Berger (2001), Soil moisture retrieval from space: The Soil Moisture and Ocean Salinity (SMOS) mission, *IEEE Trans. Geosci. Remote Sens.*, *39*(8), 1729–1735.

Le Hégarat-Mascle, S., M. Zribri, F. Elem, A. Weisse, and C. Loumagne (2002), Soil moisture estimation from ERS/SAR data: Toward an operational methodology, *IEEE Trans. Geosci. Remote Sens.*, *40*(12), 2647–2658.

Loew, A. (2008), Impact of surface heterogeneity on surface soil moisture retrievals from passive microwave data at the regional scale: The Upper Danube case, *Remote Sens. Environ.*, *112*, 231–248, doi:10.1016/j.rse.2007.04.009.

Loew, A., and W. Mauser (2007), Generation of geometrically and radiometrically terrain corrected SAR image products, *Remote Sens. Environ.*, *106*(3), 337–349, doi:10.1016/j.rse.2006.09.002.

Loew, A., and W. Mauser (2008a), On the disaggregation of passive microwave soil moisture data using a priori knowledge of temporal persistent soil moisture fields, *IEEE Trans. Geosci. Remote Sens.*, *46*(3), 819–834.

Loew, A., and W. Mauser (2008b), Inverse modeling of soil characteristics from surface soil moisture observations: Potential and limitations, *Hydrol. Earth Syst. Sci. Discuss.*, *5*, 1–51.

Loew, A., R. Ludwig, and W. Mauser (2006), Derivation of surface soil moisture from ENVISAT ASAR wideswath and image mode data in agricultural areas, *IEEE Trans. Geosci. Remote Sens.*, *44*(4), 889–899.

Loew, A., H. Bach, and W. Mauser (2007), 5 years of ENVISAT ASAR soil moisture observations in southern Germany, in *Proc. ENVISAT Symposium 23–27.04.2007*, *ESA-SP636*, Montreux, Switzerland.

Loew, A., M. Schwank, and F. Schlenz (2009), Assimilation of an L-band microwave soil moisture proxy to compensate for uncertainties in precipitation data, *IEEE Trans. Geosci. Remote Sens.*, in press.

Ludwig, R., and W. Mauser (2000), Modelling catchment hydrology within a GIS-based SVAT model framework, *Hydrol. Earth Syst. Sci.*, *4*(2), 239–249.

Luterbacher, J., D. Dietrich, E. Xoplaki, M. Grosjean, and H. Wanner (2004), European seasonal and annual temperature variability, trends and extremes since 1500, *Science*, *303*, 1499–1503.

Mätzler, C., and A. Standley (2000), Relief effects for passive microwave remote sensing, *Int. J. Remote Sens.*, *21*(12), 2403–2412.

Mauser, W., and S. Schädlich (1998), Modelling the spatial distribution of evapotranspiration using remote sensing data and Promet, *J. Hydrol.*, *213*, 250–267.

Meehl, G. A., and C. Tebaldi (2004), More intense, more frequent, and longer lasting heat waves in the 21st century, *Science*, *305*, 994–997.

Meesters, A. G. C. A., R. de Jeu, and M. Owe (2005), Analytical derivation of the vegetation optical depth from the microwave polarization difference index, *IEEE Geosci. Remote Sens. Lett.*, *2*(2), 121–123.

Mialon, A., L. Coret, Y. Kerr, F. Secherre, and J.-P. Wigneron (2008), Flagging the topographic impact on the SMOS signal, *IEEE Trans. Geosci. Remote Sens.*, *46*(3), 689–694.

Monteith, J. (1965), Evaporation and the environment, in *Proc. Symposium of the Society of Exploratory Biology*, vol. 19, pp. 205–234.

Muerth, M. (2008), A multiscale energy balance and soil temperature model to assess water related climate change impacts, Ph.D. thesis, Univ. of Munich, Germany.

MunichRe (2008), MRNatCatService, MunichRe, Munich, Germany.

Njoku, E., T. Jackson, V. Lakshmi, T. Chan, and S. V. Nghiem (2003), Soil moisture retrieval from AMSRE, *IEEE Trans. Geosci. Remote Sens.*, *41*(2), 215–229.

Owe, M., R. de Jeu, and T. Holmes (2008), Multi-sensor historical climatology of satellite-derived global land surface moisture, *J. Geophys. Res.*, *113*, F01002, doi:10.1029/2007JF000769.

Pauwels, V. R. N., W. Timmermans, and A. Loew (2008), Comparison of the estimated water and energy budgets of a large winter wheat field during AGRISAR 2006 by multiple sensors and models, *J. Hydrol.*, *349*, 425–440.

Philip, J. (1957), The theory of infiltration. I: The infiltration equation and its solution, *Soil Sci.*, *83*, 345–357.

Picard, G., T. Le Toan, and F. Mattia (2003), Understanding C-band radar backscatter from wheat canopy using a multiple-scattering coherent model, *IEEE Trans. Geosci. Remote Sens.*, *41*(7), 1583–1591.

Reichle, R., D. McLaughlin, and D. Entekhabi (2002), Hydrological data assimilation with the Ensemble Kalman Filter, *Mon. Weather Rev.*, *130*, 103–114.

Reichle, R., R. Koster, P. Liu, S. Mahanama, E. Njoku, and M. Owe (2007), Comparison and assimilation of global soil moisture retrievals from the advanced microwave scanning radiometer for the earth observing system (AMSR-E) and the scanning multichannel microwave radiometer (SMMR), *J. Geophys. Res.*, *112*, D09108, doi:10.1029/2006JD008033.

Rüdiger, C., J.-C. Calvet, C. Gruhier, T. Holmes, R. de Jeu, and W. Wagner (2009), An intercomparison of ERS-Scat and AMSR-E observations, and soil moisture simulations over France, *J. Hydrometeor.*, doi:10.1175/2008JHM997.1, in press.

Sahr, K., D. White, and A. J. Kimerling (2003), Geodesic discrete global grid systems, *Cartogr. Geogr. Inf. Sci.*, *30*(2), 121–134.

Santanello, J. A., C. D. Peters-Lidard, M. E. Garcia, D. M. Mocko, M. A. Tischler, S. Moran, and D. Thoma (2007), Using remotely-sensed estimates of soil moisture to infer soil texture and hydraulic properties across a semi-arid watershed, *Remote Sens. Environ.*, *110*, 79–97.

Schär, C., and G. Jendritzky (2004), Climate change: Hot news from summer 2003, *Nature*, *432*, 559–560.

Schär, C., P. L. Vidale, D. Lüthi, C. Frei, C. Häberli, M. A. Liniger, and C. Appenzeller (2004), The role of increasing temperature variability in European summer heatwaves, *Nature*, *427*, 332–336.

Schneider, K. (2003), Assimilating remote sensing data into a land-surface process model, *Int. J. Remote Sens.*, *23*(14), 2959–2980.

Schneider, U., T. Fuchs, A. Meyer-Christoffer, and B. Rudolf (2008), *Global Precipitation Analysis Products of the GPCC. Global Precipitation Climatology Centre (GPCC)*, DWD Internet Publication, pp. 1–12. (Available at http://www.dwd.de/)

Schwank, M., C. Mätzler, M. Guglielmetti, and H. Flüher (2005), L-band radiometer measurements of soil water under growing clover grass, *IEEE Trans. Geosci. Remote Sens.*, *43*(10), 2225–2237.

Stolz, R., M. Braun, M. Probeck, R. Weidinger, and W. Mauser (2005), Land use classification in complex terrain: The role of ancillary knowledge, *EARSeL eProc.*, *4*(1), 94–105.

Strasser, U., and W. Mauser (2001), Modelling the spatial and temporal variations of the water balance for the Weser catchment 1965–1994, *J. Hydrol.*, *254*(1–4), 199–214.

Vautard, R. (2007), Summertime European heat and drought waves induced by wintertime Mediterranean rainfall deficit, *Geophys. Res. Lett.*, *34*, L07711, doi:10.1029/2006GL028001.

Wagner, W., G. Blschl, P. Pampaloni, J.-C. Calvet, B. Bizzarri, J.-P. Wigneron, and Y. Kerr (2007a), Operational readiness of microwave

remote sensing of soil moisture for hydrologic applications, *Nord. Hydrol.*, *38*(1), 1–20.

Wagner, W., V. Naeimi, K. Scipal, R. de Jeu, and J. Martínez-Fernández (2007b), Soil moisture from operational meteorological satellites, *Hydrogeol. J.*, *15*, 121–131.

Wagner, W., C. Pathe, M. Doubkova, D. Sabel, A. Bartsch, S. Hasenauer, G. Blöschl, J. Martinez-Fernandez, and A. Loew (2008), Temporal stability of soil moisture and radar backscatter observed by the Advanced Synthetic Aperture Radar (ASAR), *Sens. J.*, *8*, 1174–1197.

Walker, J., G. Willgoose, and J. Kalma (2001), One-dimensional soil moisture profile retrieval by assimilation of near-surface observations: A comparison of retrieval algorithms, *Adv. Water Resour.*, *24*, 631–650.

Wigneron, J.-P., J.-C. Calvet, T. Pellarin, A. A. Van de Griend, M. Berger, and P. Ferrazzoli (2003), Retrieving near-surface soil moisture from microwave radiometric observations: Current status and future plans, *Remote Sens. Environ.*, *85*, 489–506.

Wigneron, J.-P., J. Calvet, P. de Rosnay, Y. Kerr, P. Waldteufel, K. Saleh, M. Escorihuela, and A. Kruszewski (2004), Soil moisture retrievals from biangular L-band passive microwave observations, *IEEE Trans. Geosci. Remote Sens.*, *1*(2), 277–281.

Zaitchik, B. F., A. K. Macaldy, L. R. Bonneau, and R. B. Smith (2006), Europe's 2003 heat wave: A satellite view of impacts and land-atmosphere feedbacks, *Int. J. Climatol.*, *26*, 743–769.

Zribi, M., and M. Dechambre (2002), A new empirical model to retrieve soil moisture and roughness from C-band radar data, *Remote Sens. Environ.*, *84*, 42–52.

R. de Jeu and T. Holmes, Faculty of Earth and Life Sciences, Department of Hydrology and Geo-environmental Sciences, Vrije Universiteit Amsterdam, De Boelelaan 1085, 1081 HV Amsterdam, Netherlands.

A. Loew, Max-Planck-Institute for Meteorology, The Land in the Earth System, Bundesstr. 53, 20146 Hamburg, Germany. (alexander.loew@zmaw.de)